Measurement 190 (2022) 110656

Contents lists available at ScienceDirect

Measurement

journal homepage: www.elsevier.com/locate/measurement

Determination of error-corrected full scattering parameters of a two-port device from uncalibrated measurements

Ugur Cem Hasar [a,*], Hamdullah Ozturk [a], Huseyin Korkmaz [a], Mucahit Izginli [a,b], Mona Sadat Sophi Alfaqawi [a], Omar Mustafa Ramahi [c]

[a] *Department of Electrical and Electronics Engineering, Gaziantep University, Gaziantep, 27310, Turkey*
[b] *Department of Electrical and Electronics Engineering, Hasan Kalyoncu University, Gaziantep 27410, Turkey*
[c] *University of Waterloo, Department of Electrical and Computer Engineering, Waterloo, ON N2L 3G1, Canada*

ARTICLE INFO

Keywords:
S-parameters
Reflection-asymmetric
Non-reciprocal
Two-port network (device)
Uncalibrated measurements

ABSTRACT

A methodology relying on relating terms of a two-port error network to the scattering (S-) parameters of a two-port network or device is applied to extract its full S-parameters. The new methodology has only one sign ambiguity problem (two solutions) in evaluation of S_{11} (and thus S_{22}) while the similar methodology in the literature has two sign ambiguity problems (4 solutions). This ambiguity problem of our method is shown to be eliminated by applying an approach based on continuity of the argument of S_{11} in the frequency domain. On the other hand, our methodology, as compared with the thru-reflect-line calibration technique, does not necessitate usage of any reflection standard in determining full S-parameters of a two-port network or device. Finally, it gives information about error networks. For its validation, S-parameters of a microwave phase shifter and a polyethylene sample flushed with the left/bottom terminal of the coaxial cell were extracted.

1. Introduction

Error-corrected scattering (S-) parameters of a microwave two-port device can be obtained by using a proper calibration procedure such as the thru-reflect-line (TRL) [1], multiline TRL [2], and the thru-reflect-match [3]. To achieve the same goal, de-embedding line-line techniques can be applied for characterization of S-parameters of a two-port device [4–7], which is our main concern in this study, in addition to the determination of line impedance [8,9], line propagation constant [10–13], and complex permittivity/permeability of sample-loaded line [14–21].

In the study [4], S-parameters of a two-port network or device were determined by using connections of a thru, a non-reflecting line and the device (direct configuration). As a variant of this study [5], a non-reflecting line was used in replace of the thru connection, and the device was positioned at the mid-point of this non-reflecting line. However, these studies were limited to two-port networks or devices with reflection-symmetric property only. To extend these studies for two-port networks or devices with asymmetric reflections (as well as symmetric reflections), we have proposed two different techniques [6, 7]. In the first technique [6], direct and reversed configurations of the two-port network or device in addition to thru and non-reflecting line configurations were utilized to extract full S-parameters. Although forward and backward transmission properties S_{21} and S_{12} were determined with no difficulty, forward and backward reflection properties had the problem of sign ambiguity. Specifically, there are four solutions for evaluating the forward reflection S-parameter S_{11} (and thus the backward reflection S-parameter S_{22}), and there is no specific criterion for ascertaining the correct one among these possible solutions. In other words, application of the criterion $|S_{11}| \leq 1.0$ does not resolve the problem where $|\star|$ denotes the magnitude operation. On the other hand, in the second technique [7], configurations of the device itself and the same device on a reference material whose properties are known, along with configurations of thru and non-reflecting line, were used to characterize the two-port network or device. Nonetheless, this second technique likewise requires the knowledge of reflection and transmission S-parameters of the reference material or necessitates that the reference material be reflection-symmetric and transmission-symmetric if its S-parameters are not known priori. It is for sure that any inaccurate information about S-parameters of the reference material will seriously affect the accuracy of this second technique. Additionally, at some frequencies, it is not possible to separate the two possible solutions for S_{11} of the two-port network or device because the common criterion $|S_{11}| \leq 1.0$ is not useful. Furthermore, any small gap between the reference material and the device could drastically

* Corresponding author.
E-mail address: uchasar@gantep.edu.tr (U.C. Hasar).

https://doi.org/10.1016/j.measurement.2021.110656
Received 5 August 2021; Received in revised form 14 December 2021; Accepted 23 December 2021
Available online 10 January 2022

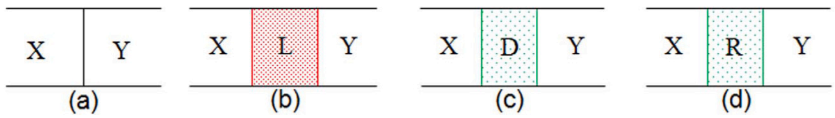

Fig. 1. Four different configurations for evaluating full S-parameters of a two-port network or device. (a) Thru connection, (b) non-reflecting line (denoted by the letter 'L') connection, (c) direct connection of the device (denoted by the letter 'D'), and (d) reversed connection of the device (denoted by the letter 'R').

degrade the performance of this second technique because it is not always possible to integrate a reference material next to the device due to fabrication constraints.

In this study, we revisit the problem of characterization of full S-parameters of a two-port network or device and reformulate this problem by first attacking to determination of unknown error networks and then characterization of the two-port network or device, as different from the previous studies [4–7] which directly focus on characterization of the two-port network or device without resorting to error networks. Besides, as an advantage of such an analysis, it is shown that it is possible to extract some information about the error network in addition to full characterization of the two-port network or device. Furthermore, it is demonstrated that there is only one sign ambiguity problem in evaluation of S_{11} (and thus S_{22}) using thru, non-reflecting line, direct device, and reversed device configurations without using any reference material, and this ambiguity could be eliminated by applying an approach based on continuity of their arguments in the frequency domain.

2. Proposed formalism

Fig. 1 demonstrates four different configurations for evaluating S_{11}, S_{21}, S_{12}, and S_{22} of a two-port network or device. While Fig. 1(a) depicts the thru configuration where the error networks X and Y are connected together, Fig. 1(b) depicts the non-reflecting line configuration (denoted by the letter 'L') sandwiched between X and Y. Figs. 1(c) and 1(d) depict, respectively, the direct configuration (denoted by the letter 'D') and the reversed configuration (denoted by the letter 'R') of the device in between X and Y.

2.1. Wave cascading matrices

According to the 8-term error matrix description [1], the wave cascading matrices (WCMs) of the configurations M_a, M_b, M_c, and M_d in Figs. 1(a)–(d) can be written as

$$M_a = T_X T_Y, \quad M_b = T_X T_{nr} T_Y, \quad M_c = T_X T_D T_Y, \quad M_d = T_X T_R T_Y, \tag{1}$$

where T_X an T_Y are the WCMs of X and Y; T_{nr}, T_D, and T_R are the WCMs of the non-reflecting line, the direct configuration of the device, and the revised configuration of the device, respectively.

The WCMs M_a, M_b, M_c, and M_d are related to the measured forward and backward reflection and transmission S-parameters S_{11u}, S_{21u}, S_{12u}, and S_{22u} by

$$M_u = \frac{1}{S_{21u}} \begin{bmatrix} (S_{21u} S_{12u} - S_{11u} S_{22u}) & S_{11u} \\ -S_{22u} & 1 \end{bmatrix}, \tag{2}$$

where $u = a$, b, c, or d.

The expressions of the WCMs of T_{nr}, T_D, and T_R are determined for $\exp(+i\omega t)$ as

$$T_{nr} = \begin{bmatrix} T_0 & 0 \\ 0 & 1/T_0 \end{bmatrix}, \tag{3}$$

$$T_D = \frac{1}{S_{21}} \begin{bmatrix} S_{21} S_{12} - S_{11} S_{22} & S_{11} \\ -S_{22} & 1 \end{bmatrix} = \frac{1}{S_{21}} \begin{bmatrix} -\Delta & S_{11} \\ -S_{22} & 1 \end{bmatrix}, \tag{4}$$

$$T_R = \frac{1}{S_{12}} \begin{bmatrix} S_{12} S_{21} - S_{22} S_{11} & S_{22} \\ -S_{11} & 1 \end{bmatrix} = \frac{1}{S_{12}} \begin{bmatrix} -\Delta & S_{22} \\ -S_{11} & 1 \end{bmatrix}, \tag{5}$$

where

$$T_0 = e^{-\gamma_0 L_{nr}}, \quad \Delta = S_{11} S_{22} - S_{21} S_{12}, \tag{6}$$

and γ_0 and L_{nr} are the propagation constant and the length of the non-reflecting line.

2.2. The error matrix T_X

Expressing the error matrix T_X [11] as

$$T_X = \kappa \begin{bmatrix} \chi_1 & \chi_2 \\ \chi_3 & 1 \end{bmatrix}, \tag{7}$$

it is possible to relate measurement quantities $M_b M_a^{-1}$, $M_c M_a^{-1}$, $M_c M_b^{-1}$, and $M_d M_a^{-1}$ by

$$M_b M_a^{-1} = T_X T_{nr} T_X^{-1} = \begin{bmatrix} u_{11} & u_{12} \\ u_{21} & u_{22} \end{bmatrix}, \tag{8}$$

$$M_c M_a^{-1} = T_X T_D T_X^{-1} = \begin{bmatrix} m_{11} & m_{12} \\ m_{21} & m_{22} \end{bmatrix}, \tag{9}$$

$$M_d M_a^{-1} = T_X T_R T_X^{-1} = \begin{bmatrix} p_{11} & p_{12} \\ p_{21} & p_{22} \end{bmatrix}, \tag{10}$$

where κ, χ_1, χ_2, and χ_3 are the terms of the unknown T_X; u_{11}, u_{21}, u_{12}, u_{22}, m_{11}, m_{21}, m_{12}, m_{22}, n_{11}, n_{21}, n_{12}, n_{22}, p_{11}, p_{21}, p_{12}, and p_{22} are the known terms evaluated from measured M_a, M_b, M_c, and M_d.

2.3. Relating error terms to S-parameters

Using the expressions in (8)–(10), one can determine

$$T_{nr} = \begin{bmatrix} T_0 & 0 \\ 0 & 1/T_0 \end{bmatrix} = \frac{1}{(\chi_1 - \chi_2 \chi_3)} \times \begin{bmatrix} \chi_3 \left[(u_{11} - u_{21}\chi_2) \dfrac{\chi_1}{\chi_3} + (u_{12} - u_{22}\chi_2) \right] & -\left[u_{21}\chi_2^2 + (u_{22} - u_{11})\chi_2 - u_{12} \right] \\ \chi_3^2 \left[u_{21} \left(\dfrac{\chi_1}{\chi_3} \right)^2 + (u_{22} - u_{11}) \dfrac{\chi_1}{\chi_3} - u_{12} \right] & \chi_3 \left[(u_{22} + u_{21}\chi_2) \dfrac{\chi_1}{\chi_3} - (u_{12} + u_{11}\chi_2) \right] \end{bmatrix} \tag{11}$$

$$T_D = \frac{1}{S_{21}} \begin{bmatrix} -\Delta & S_{11} \\ -S_{22} & 1 \end{bmatrix} = \frac{1}{(\chi_1 - \chi_2 \chi_3)} \times \begin{bmatrix} \chi_3 \left[(m_{11} - m_{21}\chi_2) \dfrac{\chi_1}{\chi_3} + (m_{12} - m_{22}\chi_2) \right] & -\left[m_{21}\chi_2^2 + (m_{22} - m_{11})\chi_2 - m_{12} \right] \\ \chi_3^2 \left[m_{21} \left(\dfrac{\chi_1}{\chi_3} \right)^2 + (m_{22} - m_{11}) \dfrac{\chi_1}{\chi_3} - m_{12} \right] & \chi_3 \left[(m_{22} + m_{21}\chi_2) \dfrac{\chi_1}{\chi_3} - (m_{12} + m_{11}\chi_2) \right] \end{bmatrix} \tag{12}$$

$$T_R = \frac{1}{S_{12}} \begin{bmatrix} -\Delta & S_{22} \\ -S_{11} & 1 \end{bmatrix} = \frac{1}{(\chi_1 - \chi_2 \chi_3)} \times \begin{bmatrix} \chi_3 \left[(p_{11} - p_{21}\chi_2) \dfrac{\chi_1}{\chi_3} + (p_{12} - p_{22}\chi_2) \right] & -\left[p_{21}\chi_2^2 + (p_{22} - p_{11})\chi_2 - p_{12} \right] \\ \chi_3^2 \left[p_{21} \left(\dfrac{\chi_1}{\chi_3} \right)^2 + (p_{22} - p_{11}) \dfrac{\chi_1}{\chi_3} - p_{12} \right] & \chi_3 \left[(p_{22} + p_{21}\chi_2) \dfrac{\chi_1}{\chi_3} - (p_{12} + p_{11}\chi_2) \right] \end{bmatrix} \tag{13}$$

2.4. Determining S-parameters of a general device

It is seen from (11)–(13) that S_{11}, S_{21}, S_{12}, and S_{22} are all functions of the terms χ_2 and χ_2/χ_3. Therefore, it is meaningful first to evaluate these terms. Toward this end, we obtain from the null entries of T_L in (11) the following quadratic equations for χ_2 and χ_2/χ_3:

$$u_{21}\chi_2^2 + (u_{22} - u_{11})\chi_2 - u_{12} = 0, \tag{14}$$

$$u_{21}\left(\frac{\chi_1}{\chi_3}\right)^2+(u_{22}-u_{11})\frac{\chi_1}{\chi_3}-u_{12}=0. \quad (15)$$

Because these quadratic equations have the same coefficients, they will produce the same two solutions for χ_2 and χ_1/χ_3. The correct solution for χ_2 and χ_1/χ_3 can be ascertained by applying the constraint $|\chi_2|<|\chi_1/\chi_3|$ [1].

After, from (12), one can determine S_{21} as

$$S_{21}=\frac{\frac{\chi_1}{\chi_3}-\chi_2}{(m_{22}+m_{21}\chi_2)\frac{\chi_1}{\chi_3}-(m_{12}+m_{11}\chi_2)}. \quad (16)$$

In a similar fashion, one can extract S_{12} from (13) as

$$S_{12}=\frac{\frac{\chi_1}{\chi_3}-\chi_2}{(p_{22}+p_{21}\chi_2)\frac{\chi_1}{\chi_3}-(p_{12}+p_{11}\chi_2)}. \quad (17)$$

Next, simultaneous solution of (12) and (13) results the following expressions for evaluating S_{11} and S_{22}

$$S_{11}^2=\frac{S_{12}S_{21}\left[m_{21}\chi_2^2+(m_{22}-m_{11})\chi_2-m_{12}\right]\times\left[p_{21}\left(\frac{\chi_1}{\chi_3}\right)^2+(p_{22}-p_{11})\frac{\chi_1}{\chi_3}-p_{12}\right]}{\left(\frac{\chi_1}{\chi_3}-\chi_2\right)^2}, \quad (18)$$

$$S_{22}^2=\frac{S_{12}S_{21}\left[p_{21}\chi_2^2+(p_{22}-p_{11})\chi_2-p_{12}\right]\times\left[m_{21}\left(\frac{\chi_1}{\chi_3}\right)^2+(m_{22}-m_{11})\frac{\chi_1}{\chi_3}-m_{12}\right]}{\left(\frac{\chi_1}{\chi_3}-\chi_2\right)^2}. \quad (19)$$

Values of S_{11}^2 and S_{22}^2 can uniquely be determined from (18) and (19) once S_{21} and S_{12} are evaluated from (16) and (17). Because $S_{11}=|S_{11}|e^{\theta_{11}}=\pm\sqrt{S_{11}^2}$ and $S_{22}=|S_{22}|e^{\theta_{22}}=\pm\sqrt{S_{22}^2}$, it is possible to determine $|S_{11}|$ and $|S_{22}|$ uniquely from measured S_{11}^2 in (19) and S_{22}^2 in (20). Besides, one can evaluate from (12) and (13)

$$\Delta=-\frac{1}{2\left(\frac{\chi_1}{\chi_3}-\chi_2\right)}\left\{S_{21}\left[(m_{11}-m_{21}\chi_2)\frac{\chi_1}{\chi_3}+(m_{12}-m_{22}\chi_2)\right]+S_{12}\left[(p_{11}-p_{21}\chi_2)\frac{\chi_1}{\chi_3}+(p_{12}-p_{22}\chi_2)\right]\right\}. \quad (20)$$

This means that if θ_{11} could be evaluated, θ_{22} could be automatically and uniquely computed using the constraint $S_{11}S_{22}=\Delta+S_{21}S_{12}$. A procedure for evaluating θ_{11} is presented in next subsection.

2.5. Application of the continuity approach for evaluating the argument of S_{11}

To determine unique solutions for S_{11} (and thus S_{22}), one can apply the approach of continuity in the argument of extracted S_{11} and determine unique solutions for S_{11} (and thus S_{22}) through (6) and (20)) [10,22–25]. According to this approach, it is possible to evaluate unique θ_{11} by minimizing the following objective function

$$F_{\text{obj}}=\theta_{11}(f_2)-\theta_{11}(f_1)\pm 2\pi m, \quad (21)$$

where $\theta_{11}(f_2)$ and $\theta_{11}(f_1)$ are the θ values at frequencies f_1 and f_2, and m is a natural number $(0,1,2,\ldots;$ the branch index term) used to sustain the continuity of extracted θ_{11} in the frequency band. It should be mentioned that accurate determination of $\theta_{11}(f_2)$ requires the knowledge about $\theta_{11}(f_1)$, which could be supplemented if some preliminary information of electromagnetic properties of the two-port network or device at one frequency, to be discussed in Section 3, are known priori.

2.6. Determining S-parameters of a special device

It is noted that depending on the character of the two-port network or device, it is possible to specialize the above analysis. For example, for a reciprocal (but non-symmetrical reflection) case, we can obtain

$$S_{21}^{av}=\frac{S_{21}+S_{12}}{2}, \quad (22)$$

once S_{21} and S_{12} are evaluated from the expressions in (16) and (17). Besides, for a reflection-symmetric (but non-reciprocal) case, we can determine

$$S_{11}^{av}=\frac{S_{11}+S_{22}}{2}, \quad (23)$$

once S_{11} and S_{22} are evaluated from the expressions in (6) and (18)–(21). Finally, if the network or device is reflection-symmetric and reciprocal, it is possible to calculate

$$S_{11}^{av}=\frac{S_{11}+S_{22}}{2}, \quad S_{21}^{av}=\frac{S_{21}+S_{12}}{2}. \quad (24)$$

2.7. Information about error networks

In addition to the information about χ_2 and χ_1/χ_3 of the error network X using (14) and (15), it is also possible to determine some of the parameters of the error network Y. Defining

$$T_Y=\lambda\begin{bmatrix}\xi_1 & \xi_3\\ \xi_2 & 1\end{bmatrix}, \quad (25)$$

$$M_a^{-1}M_b=T_Y^{-1}T_{nr}T_Y=\begin{bmatrix}n_{11} & n_{12}\\ n_{21} & n_{22}\end{bmatrix}, \quad (26)$$

it is possible to obtain

$$T_{nr}=\begin{bmatrix}T_0 & 0\\ 0 & 1/T_0\end{bmatrix}=\frac{1}{(\xi_1-\xi_2\xi_3)}\times\begin{bmatrix}\xi_3\left[(n_{11}-n_{12}\xi_2)\frac{\xi_1}{\xi_3}+(n_{21}-n_{22}\xi_2)\right] & \xi_3^2\left[n_{12}\left(\frac{\xi_1}{\xi_3}\right)^2+(n_{22}-n_{11})\frac{\xi_1}{\xi_3}-n_{21}\right]\\ -\left[n_{12}\xi_2^2+(n_{22}-n_{11})\xi_2-n_{21}\right] & \xi_3\left[(n_{22}+n_{12}\xi_2)\frac{\xi_1}{\xi_3}-(n_{21}+n_{11}\xi_2)\right]\end{bmatrix} \quad (27)$$

and

$$n_{12}\xi_2^2+(n_{22}-n_{11})\xi_2-n_{21}=0, \quad (28)$$

$$n_{12}\left(\frac{\xi_1}{\xi_3}\right)^2+(n_{22}-n_{11})\frac{\xi_1}{\xi_3}-n_{21}=0. \quad (29)$$

The correct solution for ξ_2 and ξ_1/ξ_3 can be ascertained by applying the constraint $|\xi_2|<|\xi_1/\xi_3|$ [1]. It means that values of ξ_2 and ξ_1/ξ_3 can also be determined uniquely.

3. Measurement and discussion

Two different measurement configurations shown in Figs. 2(a) and 2(c) were used to validate our proposed formalism. For the first measurement configuration, an X-band (8.2–12.4 GHz) waveguide setup [12,13,20] was used to measure S-parameters of a waveguide phase shifter (a non-reciprocal network) loaded with ferrite material from Kearfott company with L = 28.7 mm (considered as a two-port device), as shown in Fig. 2(b), using uncalibrated S-parameters of the configurations in Fig. 1. Here, an empty waveguide section with a length of L_{nr} = 9.45 mm was used as the non-reflecting line. Two waveguide washers of 200 mm were applied to maintain propagation of the dominant mode (TE_{10}) within waveguide. For the second measurement configuration, a broadband coaxial-line measurement setup [21], which has a frequency range up to 3.0 GHz, was operated to measure S-parameters of a reciprocal Polyethylene (PE) sample with a length

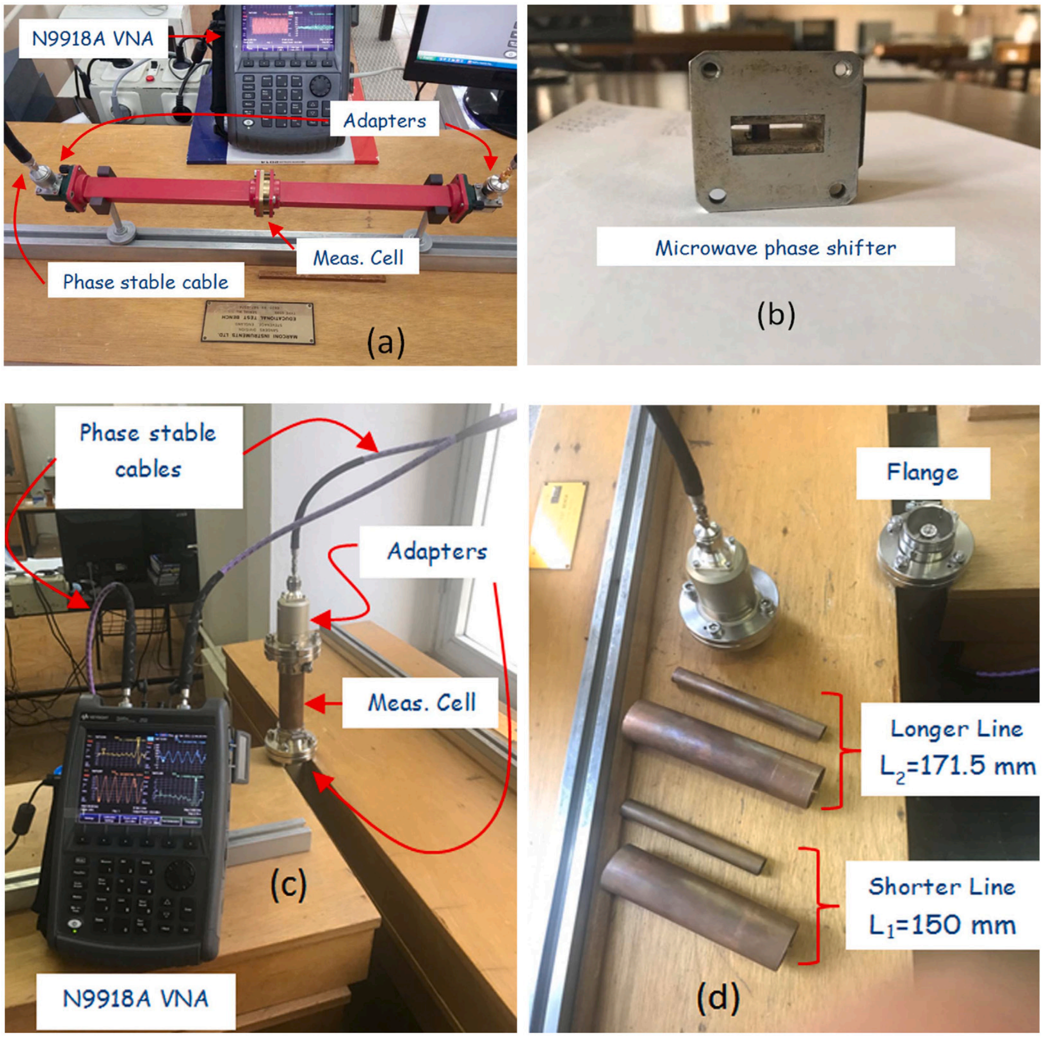

Fig. 2. Pictures of (a) the waveguide measurement setup [12,13,20], (b) the waveguide phase shifter, (c) the coaxial-line measurement setup [21], and (d) the coaxial lines and their flanges.

of 3.85 mm. Two coaxial cells with lengths of $L_1 = 150$ mm and $L_2 = 171.5$ mm (their outer and inner diameters are approximately 38.8 ∓ 0.075 mm and 16.9 ∓ 0.050 mm) were used in application of our method. Empty coaxial lines with L_1 and L_2 were connected between coaxial adapters (see Fig. 2(c)) to implement the configurations in Figs. 1(a) and 1(b), respectively ($L_{nr} = 21.5$ mm), because the reference planes of the shorter cell were assumed to be merged in the longer cell [26]. Then, the PE sample was positioned (arbitrarily) within the longer cell to measure S-parameters of the configuration in Fig. 1(c). Finally, this sample was shifted toward right (or upward, please see Fig. 2(c)) by a distance of approximately $L_{nr}-3.85 \cong 17.65$ mm to realize the configuration in Fig. 1(d). In reference to the measurement configurations in Figs. 1(a)-1(d), these coaxial line connections eventually could be used to measure full S-parameters of the PE sample flushed with the left/bottom terminal of the coaxial cell with length L_{nr}. For both measurement configurations, a vector network analyzer (VNA) (N9918 A) from Keysight Technologies, which operates between 30 kHz and 26.5 GHz, was operated to measure S-parameters. In addition, two phase-stable coaxial lines with lengths of 100 cm were used to transfer electromagnetic signals from the VNA to the adapters of each configuration.

Our proposed methodology was applied to extract S_{11}, S_{21}, S_{12}, and S_{22} of the microwave phase shifter and the coaxial-line with the PE sample. Figs. 3–6 present real and imaginary parts of extracted S-parameters of this shifter. To validate our proposed methodology and compare its accuracy, its S-parameters were also measured after the waveguide setup was calibrated by the TRL technique [1]. A waveguide washer of 9.45 mm was operated as the line standard, which results in approximately $\mp 70°$ phase variation from $-90°$ at 10.3 GHz, while a highly reflective metal termination was operated as the reflect standard. Calibration process was validated by measuring S-parameters of the line standard. It was observed that $|S_{11}|$ (and $|S_{22}|$) was less than approximately -40 dB, and $|S_{21}|$ (and $|S_{12}|$) was not less than -0.03 dB. Measured calibrated S-parameters of the shifter are given in Figs. 3–6.

It is seen from Figs. 3–5 that extracted S-parameters ($|S_{11}|$, $|S_{22}|$, S_{21}, and S_{12}) by our proposed methodology and calibrated S-parameters after the TRL calibration of the microwave phase shifter are in good agreement with each other. The advantage of our proposed method is that it does not require the reflect standard in extracting these S-parameters of a two-port network or device. Besides, Figs. 6(a) and 6(b) demonstrate the frequency dependencies of θ_{11} and θ_{22} extracted by our method before (without (21)) and after (with (21)) the continuity approach was applied. In the application of this approach, information of θ_{11} was supplemented by the calibrated S_{11} at frequency $f_1 = 8.2$ GHz. It is seen from Figs. 6(a) and 6(b) that it is possible to extract accurate phases of θ_{11} and θ_{22} by our method.

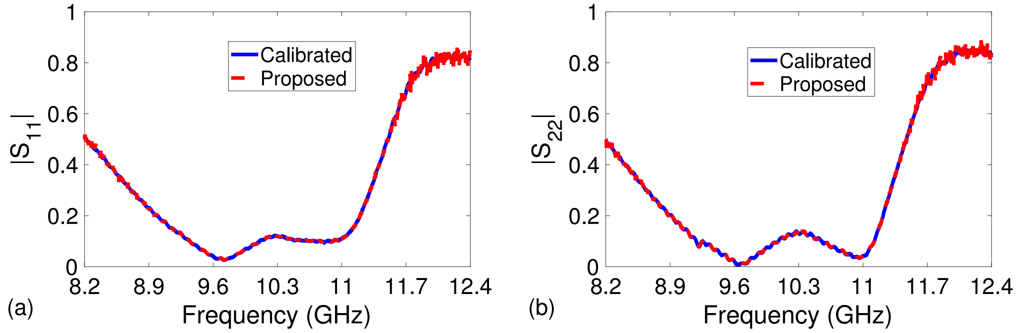

Fig. 3. (a) $|S_{11}|$ and (b) $|S_{22}|$ of the phase shifter extracted by our methodology (denoted as 'Proposed') and measured after calibration by the TRL technique (denoted as 'Calibrated').

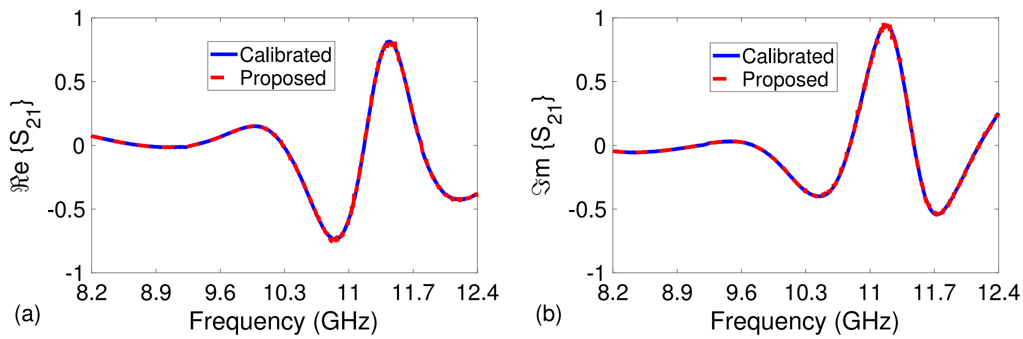

Fig. 4. (a) Real and (b) imaginary parts of S_{21} of the phase shifter extracted by our methodology (denoted as 'Proposed') and measured after calibration by the TRL technique (denoted as 'Calibrated').

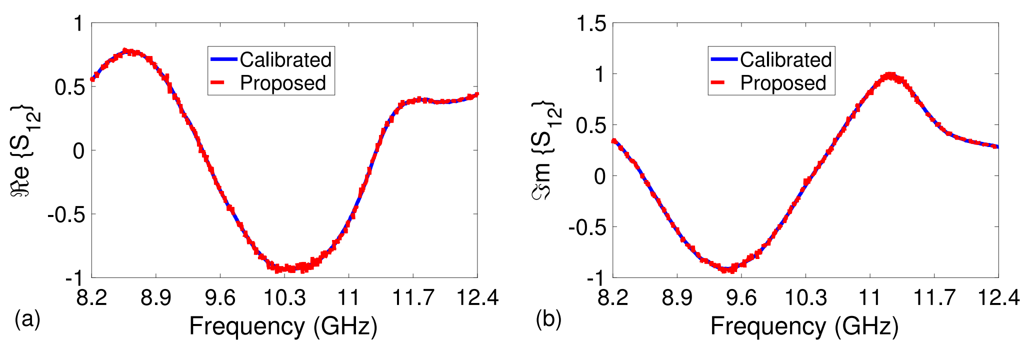

Fig. 5. (a) Real and (b) imaginary parts of S_{12} of the phase shifter extracted by our methodology (denoted as 'Proposed') and measured after calibration by the TRL technique (denoted as 'Calibrated').

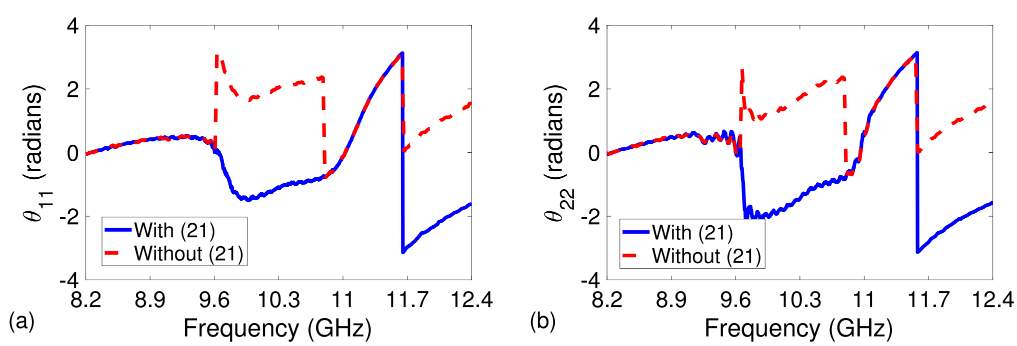

Fig. 6. Frequency dependence of (a) θ_{11} and (b) θ_{22} of the phase shifter extracted by our method before (without (21)) and after (with (21)) the continuity approach was applied.

On the other hand, Figs. 7 and 8 illustrate real and imaginary parts of extracted S_{11} and S_{21} (dependencies of S_{12} and S_{22} are not shown for brevity) of the PE sample flushed with the left/bottom terminal of the cell with length 21.5 mm. Information about θ_{11} was supplemented

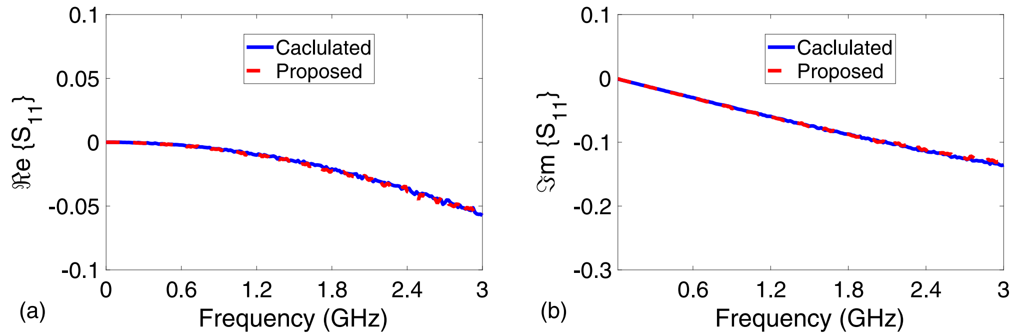

Fig. 7. (a) Real and (b) imaginary parts of S_{11} of the PE sample flushed with the left/bottom terminal of the cell with length 21.5 mm extracted by our methodology (denoted as 'Proposed') and calculated (denoted as 'Calculated') one using the reference permittivity $\varepsilon_r = 2.26 - 0.0002i$ [27].

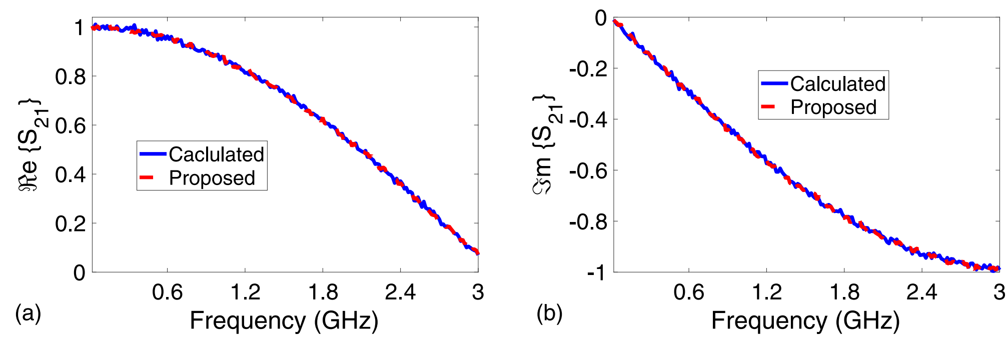

Fig. 8. (a) Real and (b) imaginary parts of S_{21} of the PE sample flushed with the left/bottom terminal of the cell with length 21.5 mm extracted by our methodology (denoted as 'Proposed') and calculated (denoted as 'Calculated') one using the reference permittivity $\varepsilon_r = 2.26 - 0.0002i$ [27].

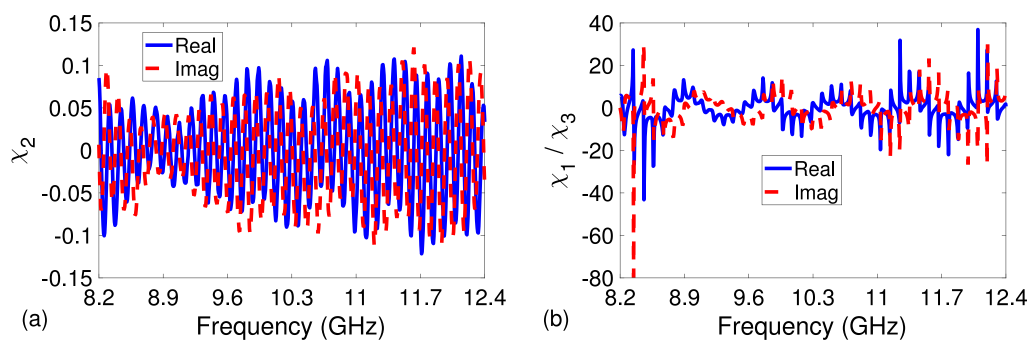

Fig. 9. Extracted real and imaginary parts of (a) χ_2 and (b) χ_1/χ_3 of the phase shifter extracted by our methodology.

at the lowest frequency (30 kHz) using the reference datum for the PE sample in the literature ($\varepsilon_r = 2.26 - 0.0002i$ at 1 kHz, 1 MHz, 100 MHz, and 3 GHz [27] where ε_r refers to the relative complex permittivity). It is noted that real and imaginary parts of the extracted S_{11} and S_{21} are in good agreement with those calculated by using this reference complex permittivity. Besides, our method, as a byproduct, can extract χ_2, χ_1/χ_3, ξ_2, and ξ_1/ξ_3 terms of the error networks T_x and T_Y. Figs. 9 and 10 illustrate the real and imaginary parts of χ_2, χ_1/χ_3, ξ_2, and ξ_1/ξ_3 terms of the phase shifter. It is seen from Figs. 9 and 10 that χ_1/χ_3 (ξ_1/ξ_3) is greater than χ_2 (ξ_2) [1].

As a final point, it should be stated that the accuracy of our proposed methodology and the accuracy of the TRL calibration technique decrease if the insertion phase of the non-reflecting line goes out of the range between −20° and −160°. Depending on the requirement, multiple non-reflecting lines with varying lengths could be utilized as a remedy for broadband measurements [2]. The non-reflecting line used in application of our method did not produce any phase problem. It should also be emphasized that the accuracy of our method can decrease if the two-port network or device has considerable loss so that magnitudes of measured transmission S-parameters are less than −40 dB and thus accuracy of these S-parameters decreases.

4. Conclusion

A new methodology has been applied to extract S_{11}, S_{21}, S_{12}, and S_{22} of a two-port network or device using uncalibrated S-parameters. There are three main advantages of this methodology. First, it does not require any reflection standard in evaluating full S-parameters. Second, there is only one sign ambiguity problem (two solutions) for the applied methodology in evaluating S_{11} or S_{22}, while another similar methodology produces two sign ambiguities (four solutions). The sign ambiguity in the extracted reflection S-parameters could be removed by applying an approach based on continuity of their arguments in the frequency domain. Third, the methodology gives information about error terms T_X and T_Y. S-parameters of a microwave phase shifter and a PE sample flushed with the left/bottom terminal of the coaxial cell with length L_{nr} were extracted to validate our proposed methodology.

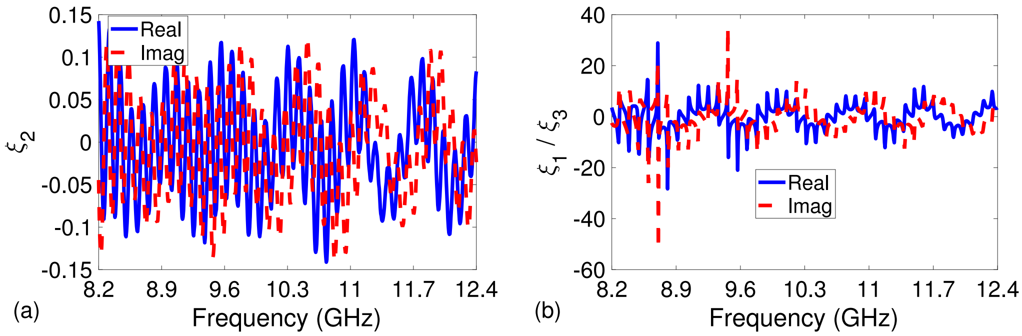

Fig. 10. Extracted real and imaginary parts of (a) ξ_2 and (b) ξ_1/ξ_3 of the phase shifter extracted by our methodology.

CRediT authorship contribution statement

Ugur Cem Hasar: Conceptualization, Methodology, Investigation, Writing – original draft. **Hamdullah Ozturk:** Visualization, Writing – review & editing. **Huseyin Korkmaz:** Visualization, Writing – review & editing. **Mucahit Izginli:** Visualization, Writing – review & editing. **Mona Sadat Sophi Alfaqawi:** Visualization. **Omar Mustafa Ramahi:** Investigation, Writing – review & editing.

Declaration of competing interest

The authors declare that they have no known competing financial interests or personal relationships that could have appeared to influence the work reported in this paper.

References

[1] G.F. Engen, C.A. Hoer, Thru-reflect-line: An improved technique for calibrating the dual 6-port automatic network analyzer, IEEE Trans. Microw. Theory Tech. 27 (12) (1979) 983–987.

[2] R.B. Marks, A multiline method of network analyzer calibration, IEEE Trans. Microw. Theory Tech. 39 (7) (1991) 1205–1215.

[3] H.J. Eul, B. Schiek, A generalized theory and new calibration procedures for network analyzer self-calibration, IEEE Trans. Microw. Theory Tech. 39 (4) (1991) 724–731.

[4] C. Wan, B. Nauwelaers, W. De Raedt, A simple error correction method for two-port transmission parameter measurement, IEEE Microw. Guided Wave Lett. 8 (2) (1998) 58–59.

[5] J. Reynoso-Hernández, C.F. Estrada-Maldonado, Broadband determination of two-port transmission (s21, s12) parameters of phemt's embedded in transmission lines, in: 55th ARFTG Conf. Dig., Vol. 37, 2000, pp. 1–4.

[6] U.C. Hasar, M. Bute, Error-corrected reflection and transmission scattering parameters of a two-port device, IEEE Microw. Wirel. Compon. Lett. 27 (7) (2017) 681–683.

[7] U.C. Hasar, Determination of full s-parameters of a low-loss two-port device from uncalibrated measurements, Rev. Sci. Instrum. 89 (12) (2018) 124701.

[8] J. Zúñiga-Juárez, J. Reynoso-Hernández, J. Loo-Yau, M. Maya-Sánchez, An improved two-tier l-l method for characterizing symmetrical microwave test fixtures, Measurement 44 (9) (2011) 1491–1498.

[9] J.A. Reynoso-Hernández, M.A. Pulido-Gaytán, R. Cuesta, J.R. Loo-Yau, M.C. Maya-Sánchez, Transmission line impedance characterization using an uncalibrated vector network analyzer, IEEE Microw. Wirel. Compon. Lett. 30 (5) (2020) 528–530.

[10] M.D. Janezic, J.A. Jargon, Complex permittivity determination from propagation constant measurements, IEEE Microw. Guided Wave Lett. 9 (2) (1999) 76–78.

[11] J.A. Reynoso-Hernández, Unified method for determining the complex propagation constant of reflecting and nonreflecting transmission lines, IEEE Microw. Wirel. Compon. Lett. 13 (8) (2003) 351–353.

[12] U.C. Hasar, Y. Kaya, G. Ozturk, M. Ertugrul, Propagation constant measurements of reflection-asymmetric and nonreciprocal microwave networks from s-parameters without using a reflective standard, Measurement 165 (2020) 108126.

[13] U.C. Hasar, Y. Kaya, M. Ertugrul, Measurement of propagation characteristics of nonreciprocal networks/lines using a line-line method, IEEE Trans. Electromagn. Compat. (2020) 1–8.

[14] C. Wan, B. Nauwelaers, W.D. Raedt, M.V. Rossum, Complex permittivity measurement method based on asymmetry of reciprocal two-ports, Electron. Lett. 32 (16) (1996) 1497–1498.

[15] C. Wan, B. Nauwelaers, W.D. Raedt, M.V. Rossum, Two new measurement methods for explicit determination of complex permittivity, IEEE Trans. Microw. Theory Tech. 46 (11) (1998) 1614–1619.

[16] I. Huynen, C. Steukers, F. Duhamel, A wideband line-line dielectrometric method for liquids, soils, and planar substrates, IEEE Trans. Instrum. Meas. 50 (5) (2001) 1343–1348.

[17] C. Guoxin, Calibration-independent measurement of complex permittivity of liquids using a coaxial transmission line, Rev. Sci. Instrum. 86 (1) (2015) 014704.

[18] X. Bao, S. Liu, I. Ocket, J. Bao, D. Schreurs, S. Zhang, C. Cheng, K. Feng, B. Nauwelaers, A general line-line method for dielectric material characterization using conductors with the same cross-sectional geometry, IEEE Microw. Wirel. Compon. Lett. 28 (4) (2018) 356–358.

[19] U.C. Hasar, Self-calibrating transmission–reflection technique for constitutive parameters retrieval of materials, IEEE Trans. Microw. Theory Tech. 66 (2) (2018) 1081–1089.

[20] U.C. Hasar, Propagation constant measurement of microwave networks with symmetric/asymmetric reflections, IEEE Sens. J. 18 (12) (2018) 4940–4946.

[21] H. Hasar, U.C. Hasar, Y. Kaya, T. Oztas, M.Y. Canbolat, N. Aslan, M. Ertugrul, O.M. Ramahi, Broadband soil permittivity measurements using a novel de-embedding line-line method, IEEE Geosci. Remote Sens. Lett. 19 (2022) 5002605.

[22] J.J. Barroso, U.C. Hasar, Constitutive parameters of a metamaterial slab retrieved by the phase unwrapping method, J. Infrared Milli Terahz Waves 33 (2012) 237–244.

[23] U.C. Hasar, J.J. Barroso, C. Sabah, Y. Kaya, M. Ertugrul, Stepwise technique for accurate and unique retrieval of electromagnetic properties of bianisotropic metamaterials, J. Opt. Soc. Amer. B 30 (2013) 1058–1068.

[24] Y. Shi, Z.-Y. Li, L. Li, C.-H. Liang, An electromagnetic parameters extraction method for metamaterials based on phase unwrapping technique, Waves Random Complex Media 26 (4) (2016) 417–433.

[25] G. Angiulli, M. Versaci, Retrieving the effective parameters of an electromagnetic metamaterial using the nicolson-ross-weir method: an analytic continuation problem along the path determined by scattering parameters, IEEE Access 9 (2021) 77511–77525.

[26] K.-F. Fuh, Broadband continuous extraction of complex propagation constants in methods using two-line measurements, IEEE Microw. Wirel. Compon. Lett. 23 (12) (2013) 671–673.

[27] G.Y. Chin, E.A. Mechtly, Properties of Materials, Howard W. Sams Co., Indianapolis, 1986, p. 420, 423.